Energy & Environmental Science

Cite this: *Energy Environ. Sci.*, 2012, **5**, 7060

www.rsc.org/ees

PAPER

Low band gap liquid-processed CZTSe solar cell with 10.1% efficiency

Santanu Bag, Oki Gunawan, Tayfun Gokmen, Yu Zhu, Teodor K. Todorov and David B. Mitzi*

Received 7th January 2012, Accepted 23rd February 2012
DOI: 10.1039/c2ee00056c

A low band gap liquid-processed $Cu_2ZnSn(Se_{1-x}S_x)_4$ (CZTSSe) kesterite solar cell with $x \approx 0.03$ is prepared from earth abundant metals, yielding 10.1% power conversion efficiency. This champion cell shows a band gap of 1.04 eV, higher minority-carrier lifetime, lower series resistance and lower Voc deficit compared to our previously reported higher band gap ($E_g = 1.15$ eV; $x \approx 0.4$) cell with similar record efficiency. The ability to vary the CZTSSe band gap using sulfur content (*i.e.*, varying x) facilitates the examination of factors limiting performance in the current generation of CZTSSe devices, as part of the thrust to achieve operational parity with CdTe and $Cu(In,Ga)(S,Se)_2$ (CIGSSe) analogs.

Introduction

Chalcogenide-based thin film solar cells are expected to form the foundation of next generation photovoltaic (PV) technology.[1] Research in this field has increased significantly due to the promise of this technology to provide cleaner energy at a cost that is competitive with fossil fuels. Among these technologies, $Cu(In,Ga)(S,Se)_2$ (CIGSSe) and CdTe solar cells are already in production with record cell efficiencies of 20.3% and 17.3%,[2,3] respectively, while their commercial modules correspondingly reach efficiencies of as high as 15.7% and 13.5%.[3,4] However, the use of toxic Cd and the nonabundant and/or expensive elements In, Ga and Te already presents a concern with respect to meeting the multi-terawatt-scale production needed in order to satisfy global energy demand.[5,6]

Recently, kesterite-structured copper zinc tin chalcogenide (sulfide/selenide) materials (collectively labeled CZTSSe) have emerged as a potential alternative to CIGSSe because of more earth abundant and less expensive constituents. The first reported CZTS ($x = 1$) solar cell was vacuum deposited with power conversion efficiency of 0.66%.[7] By 2008, optimization of deposition conditions and annealing parameters led to efficiencies of as high as 6.8% for vacuum-based CZTS.[8] More recently, 9.7% (10.1% after optimization)[9,10] power conversion efficiency has been achieved for a mixed S and Se system using a hydrazine-based processing approach, which involves a combination of solution- and nanoparticle-based deposition routes. A 7.2% power conversion efficiency has also been demonstrated with devices prepared using a colloidal nanocrystal-based approach.[11] These early-stage development results point towards a substantial promise with respect to commercialization potential for CZTSSe, if efficiency can continue to be pushed beyond 10%.

Control over band gap in chalcogenide-based solar cells is important in terms of tailoring the properties of the absorber layer to match the incident solar radiation spectrum and to otherwise optimize the device efficiency.[12–14] Like for the CIGSSe material, the band gap in CZTSSe can be tailored using the S:Se ratio.[15,16] A recent first-principle calculation report shows that

IBM T. J. Watson Research Center, 1101 Kitchawan Rd, Yorktown Heights, NY, 10598, USA. E-mail: dmitzi@us.ibm.com; Tel: (+1) 914-945-4176

Broader context

Given the remarkable potential of photovoltaic (PV) technology to displace non-renewable electricity generation based on fossil fuels if associated manufacturing costs can be made competitive, there is a tremendous need for low-cost, environmentally benign materials and fabrication processes for preparing high-performance solar cells. In this regard, thin-film heterojunction PV devices are particularly interesting because of their reduced material utilization and simple cell design. In thin-film devices, a wide range of semiconducting materials can be used as the solar absorber, among which the kesterite $Cu_2ZnSn(Se_{1-x}S_x)_4$ (CZTSSe) family has been getting significant recent attention due to its earth-abundant and less toxic constituents. To date, the highest efficiency CZTSSe solar cell is made by a hybrid solution-particle approach, where a final heat treatment is done in a sulfur environment to fine tune the band gap. Although the [S]:[Se] ratio in CZTSSe can be used to control the band gap and to optimize device performance, in practice, reproducibly controlling the [S]:[Se] ratio using a sulfur-enhanced heat treatment presents challenges because of the high volatility of sulfur. In this manuscript, we report a simplified approach to making a record 10.1% efficiency low band gap CZTSe solar cell, without any treatment in a sulfur rich atmosphere.

CZTSSe alloys with high Se content are expected to have more facile *n*- and p-type doping.[17] Based on this, it has been proposed that higher efficiency CZTSSe solar cells should be achievable with high Se content. Additionally, by focusing on a high (essentially pure) Se-content device, processing can be simplified, since control over S:Se ratio during fabrication is no longer necessary. Volatility of S and Se during heat treatments renders reproducible control over the ratio of these elements difficult to achieve for intermediate S content samples. Here we will show the fabrication of a highly selenium-enriched low band gap CZTSe solar cell and describe the device characterisitics, including high power conversion efficiency of 10.1%, which matches the performance of the recently reported higher band gap (higher S content) record device.[10]

Experimental

The absorber layer, CZTSe, used to fabricate the champion solar cell in this study was prepared using a hybrid solution-particle approach in hydrazine. The current procedure is slightly modified from a previously reported process (no extra elemental chalcogen was added during the final heat treatment).[9] All commercially available chemicals (99.998% S from Sigma Aldrich, 99.9% Zn from Strem Chemical, 99.999% SnSe from Alfa Aesar, 99.999% Se from Alfa Aesar, and 99.9% hydrazine from Arch Chemicals) were used as received, except for Cu_2S, which was synthesized in-house. All elemental metal and binary metal chalcogenides were dissolved in hydrazine (except for the elemental Zn, which remained as a particle species) before spinning onto Mo-coated soda lime glass slides ($1'' \times 1''$) and heat treating in an oxygen and water free nitrogen-filled glove box (H_2O and O_2 levels maintained below 1 ppm). *Caution*: *Hydrazine is extremely toxic and hazardous and must be handled with extreme care at all times using appropriate protective equipment.*

In a typical preparation, solution A (1.2 M Cu_2S–S) was made by dissolving Cu_2S and S in hydrazine. Similarly, SnSe, Se and Zn were stirred separately in hydrazine to form slurry B (0.57 M SnSe-Se; The Zn powder reacts to form zinc chalcogenide particles).[9] Solution A and slurry B were mixed together, yielding a slurry with final composition Cu/(Zn + Sn) = 0.8, Zn/Sn = 1.22 and nominal kesterite $Cu_{2-q}Zn_{1+y}Sn(S,Se)_4$ concentration of approximately 0.4 M. The thin film absorber layer with final thickness of ~2–2.5 μm was prepared by spin coating this mixture over five consecutive layers at 800 rpm and then subsequently subjecting to a short anneal on a ceramic hot plate with set point 540 °C (note that no sulfur rich environment was used in this annealing step). During the heat treatment step almost all sulfur used in the solution preparation evaporates, leaving essentially pure CZTSe phase.

The CdS buffer, ZnO window, and indium doped tin oxide (ITO) layers were subsequently deposited by chemical bath deposition and RF magnetron sputtering, respectively, giving a standard CIGS/CZTSSe device structure with a device area of approximately 0.45 cm^2, as defined by mechanical scribing. A Ni/Al collection grid and 110-nm-thick MgF_2 antireflection coating were deposited on top of the device by electron-beam evaporation.

Samples for TEM/STEM (scanning transmission electron microscopy) analysis were prepared using a FEI Helios 400 S DB-FIB. TEM images were taken using a JEOL 3000F TEM operated at 300 kV. Compositional profiles were acquired by STEM/EDX (energy dispersive X-ray spectroscopy). The electrical characterization was done employing a Xe-based light source solar simulator, equipped with light stabilization system, to provide simulated 1 sun AM1.5G illumination. A small liquid nitrogen flow cryostat that can be inserted under the solar simulator was used for temperature dependent measurement. The quantum efficiency measurement was performed using a Protoflex system equipped with a xenon light source and a monochromator with chopper running at 270 Hz. The time-resolved photoluminscence (TR-PL) measurement was performed on a finished cell using a Hamamatsu time-correlated single photon counting system. The system employed a 532 nm solid state laser with a pulse width of less than 1 ns and a repetition rate of 15 kHz.

Results and discussion

Based on earlier theoretical work[12] it has been suggested that the optimum band gap value of an absorber material for maximum solar energy conversion is approximately 1.45 eV. However, in the CIGS system it was experimentally shown that the highest efficiency was obtained for a relatively low band gap value of 1.14 eV.[13] For the wider band gap materials the attained values of Voc are much smaller than anticipated, since the rate of increasing Voc is not linear with increasing band gap, E_g, for [Ga]/([Ga] + [In]) > 0.3.[13] It is interesting to consider whether the same may be true for CZTSSe as well. The band gap of the CZTSSe absorber can be tuned either by substituting on the chalcogen site or on the metal site. In a semiconductor, substitution of a constitutent element with another smaller or larger radius element from the same column of the periodic table is commonly employed to change the band gap, without affecting significantly the overall crystal structure of the material (other than a simple shift in cell volume).

In the current study, control of the chalcogen site occupancy is targeted as a means of controlling band gap. It has been shown recently that substituting Se with smaller S in CZTSSe produces a valence edge shift to higher binding energy and an increase of the band gap–The band gap can be tuned from approximately 1.0 to 1.5 eV with increasing sulfur content.[16] A record efficiency of 10.1% was also recently obtained for a mixed selenosulfur system with a band gap of 1.15 eV.[10] One goal of the current study is to determine whether a similarly prepared device with lower band gap would have higher or lower efficiency and more globally to start to build a broader database of high quality samples with different band gaps, each prepared using the same basic approach, in order to examine the dependence of device characteristics on band gap in the CZTSSe system.

The low band gap CZTSSe device was prepared using a Cu poor (Cu/[Zn + Sn] = 0.8) and Zn rich (Zn/Sn = 1.2) composition. The previously reported higher band gap 10.1% efficiency CZTSSe device was made using a mixed sulfur and selenium composition,[10] where the band gap of the as-made CZTSSe was modulated by the introduction of sulfur during the annealing step as shown in eq (1). In that case, depending

upon the added amount of elemental sulfur, substitution of Se by S in CZTSSe takes place, but with a difficult to control amount due in part to the high volatility of elemental S. The current 10.1% efficiency device was achieved by a simple annealing procedure with no extra sulfurisation according to eq (2). During the final annealing step at 540 °C almost all sulfur used to dissolve binary metal chalcogenides evaporates and is replaced in the CZTSSe structure by excess Se from the precursor solution, leading to a highly selenium enriched CZTSSe final product. Because there is little S left in the film (estimate of $x = [S]/[S + Se] \approx 0.03$ as shown below), the material is abbreviated as CZTSe.

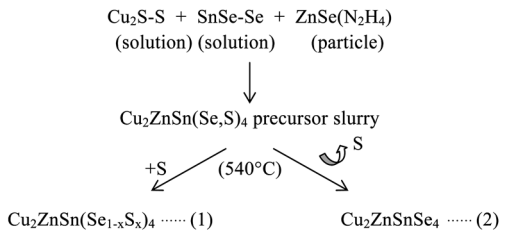

A cross-sectional transmission electron microscopy (TEM) image (Fig. 1a) of the current low band gap champion cell shows all large grains (~1.5–1.9 μm) spanning the entire CZTSe layer, with some isolated voids near the back $MoSe_2$ interface. During the annealing stage at 540 °C, Mo coated glass reacts with Se and forms the ~300 nm thick $MoSe_2$ layer. In Fig. 1b, energy dispersive X-ray (EDX) compositional profiling demonstrates negligible S content (S/[Se + S] ≈ 0.03) and uniform distribution of elements within the absorber layer. EDX line scans using STEM mode across the back interface regions reveal Cu diffusion into the $MoSe_2$ layer. Interestingly, the grain boundaries within the CZTSe absorber layer appear to be Cu rich relative to the overall Cu poor bulk film stoichiometry (Fig. 1c,d). The copper poor nature of the grain boundaries in CIGS has been proposed to be important in terms of reducing recombination at the grain boundaries.[18,19] Therefore, the copper-rich nature of the grain boundaries (consistently observed in all EDX line scans performed across grain boundaries) in this device could play an important role in terms of recombination and therefore reduction of Voc in the CZTSe device.

The electrical device characteristics of our cell under light and dark condition are presented in Fig. 2a and the external quantum efficiency curve is presented in Fig. 2b. It is useful to compare the present cell with the previous champion CZTSSe cell that we have reported (labeled as CZTSSe-1),[10] as shown in Table 1. The current cell has the same record effciency of 10.1%, but lower band gap (1.04 eV). From the device characteristics shown in Table 1, we can make a few observations. First, the present cell has lower Voc (and higher Jsc) compared to the CZTSSe-1 cell, as expected from its lower band gap (1.04 eV as opposed to 1.15 eV for the CZTSSe-1 cell). The band gap is determined from the long wavelength "absorption" edge of the external quantum efficiency curve, as shown in the Fig. 2b. It is worthwhile to observe that the present cell has a better "Voc-deficit" value (*i.e.* the difference between the absorber band gap and Voc) of 617 mV, compared to 633 mV for the CZTSSe-1 device. Voc deficit has been reported as one of the key factors limiting device performance in the current generation of CZTSSe devices.[20,21]

Another notable observation is that the present cell has lower series resistance (*cf.* $R_{SL} = 1.43\ \Omega cm^2$, Table 1) compared to the analogous higher band gap champion cell. It is also known that even higher band gap vacuum-deposited CZTS (x = 1) cells tend

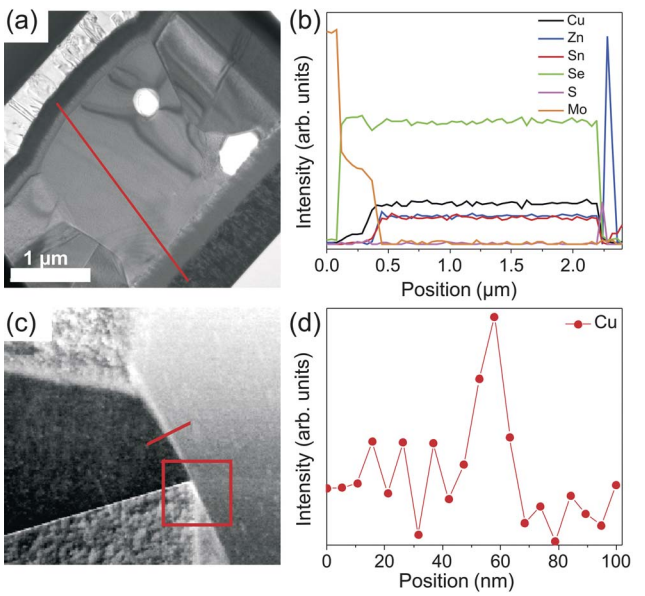

Fig. 1 (a, b) Cross-sectional TEM image and EDX line scan of the low band gap champion cell. (c, d) TEM image and EDX line scan of the same cell showing Cu rich grain boundary. In (a) and (c) the red lines denote the path examined in the EDX line scans of panels (b) and (d).

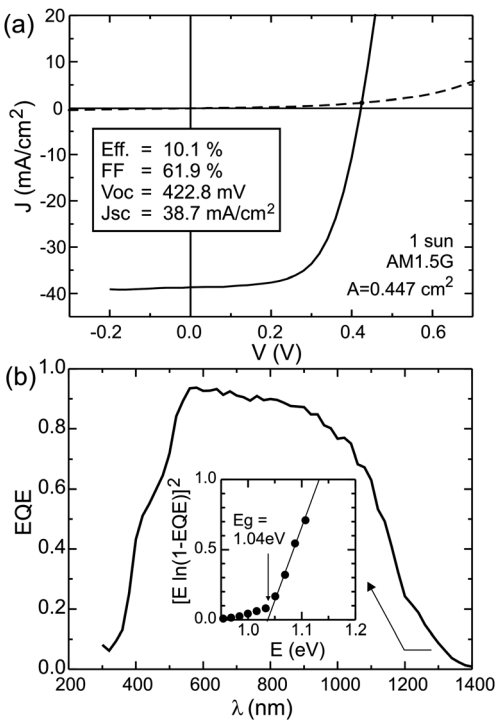

Fig. 2 (a) Light and dark J–V characteristics under simulated 1 sun AM1.5G illumination. (b) Quantum efficiency curve of the cell. Inset: band gap determination of the cell from the EQE data.

Table 1 Device characteristics[a] and comparison with the higher band gap CZTSSe-1 device[10]

Cell	η (%)	FF (%)	Voc (mV)	Eg (eV)	Eg/q-Voc (V)	Jsc (mA cm^{-2})	τ (ns)	R_{SL} Ωcm^2	A	J_0 mA cm^{-2}
CZTSSe-1	10.1	63.7	517	1.15	633	30.8	3.1	2.47	1.31	6.6e-6
Present cell	10.1	61.9	423	1.04	617	38.7	10	1.43	1.30	1.5e-4

[a] τ is the minority carrier lifetime deduced from the TR-PL study, R_{SL} is the series resistance extracted from the Light J–V and Jsc-Voc data,[28] A and J_0 are the ideality factor and reverse saturation current, respectively, extracted from the Jsc-Voc data.

to have high series resistance (*e.g.* R_{SL} = 3.4 Ωcm^2, Eg = 1.45 eV).[22] Thus this observation points to a prevailing trend that the device series resistance is lower for lower band gap absorbers in the CZTSSe system. Although the reason for this trend still remains to be determined, one possible cause is that the back contact electrical charcteristic tends to be more ohmic for a metal contact with a lower band gap absorber material. Note that, even though the present cell has lower series resistance compared to CZTSSe-1, its fill factor remains lower because Voc is significantly smaller (fill factor is expected to increase with Voc).[23]

To provide more information regarding the device characteristics in our present cell we performed temperature dependent measurement of Voc, Jsc and series resistance, as shown in Fig. 3. These measurements were performed under constant 1 sun illumination. From the Voc *vs.* temperature plot, one can extract the activation energy of the dominant recombination process, E_A, following:[24]

$$Voc = (E_A/q) - (AkT/q)\ln(J_{00}/J_L),$$

where A, J_{00} and J_L are the diode ideality factor, reverse saturation current prefactor and the photocurrent, respectively. The activation energy E_A is the 0 K intercept of the linear extrapolation of the Voc *vs.* T data plot. We obtain $E_A = 0.82$ eV for the current cell, which is significantly lower than the CZTSe layer band gap, as was also observed in previous studies on CZTSSe cells.[20,21] This low E_A in our cell is another symptom of the Voc deficit issue that we found in a broader study of CZTSSe cells of all band gaps.[21] Note that while Voc increases by ~2x from 350 K to 120 K [Fig. 3(a)], the Jsc only drops by 13%. This is mainly associated with reduction of the minority carrier diffusion length at lower temperature, which lowers the EQE.

Another relevant parameter with regards to the Voc is the minority carrier lifetime of the cell, which can be measured using time-resolved photoluminescence measurement, as shown in Fig. 4. It has been shown that the lifetime correlates with both Voc and the efficiency.[25] The lifetime extraction method has been described in ref. 25 and the TR-PL measurements were performed on a finished cell. One interesting observation is that we observe a long minority carrier lifetime of ~10 ns, which is the longest we have observed so far in CZTSSe devices. In contrast, for our previous higher band gap champion cell the lifetime was only 3.1 ns. This long minority carrier lifetime could be partly responsible for the better Voc deficit (Eg/q-Voc = 617 mV) in our present cell compared to CZTSSe-1 (Eg/q-Voc = 633 mV). Note that the TR-PL data is taken from the peak of the PL spectrum at E = 0.94 eV. This value is less than the band gap of our CZTSSe cell (Eg = 1.04 eV) as determined from the quantum efficiency data, which suggests a dominant band to impurity radiative recombination channel contributing to the PL emission.

In some reports it is shown that the minority carrier lifetime for CIGS films can be reduced in the presence of other device structure overlayers.[26] To test whether this is the case in the current device we also performed the TR-PL measurements after different processing steps for a CZTSe cell, CZTSe-B (η = 9.8%),

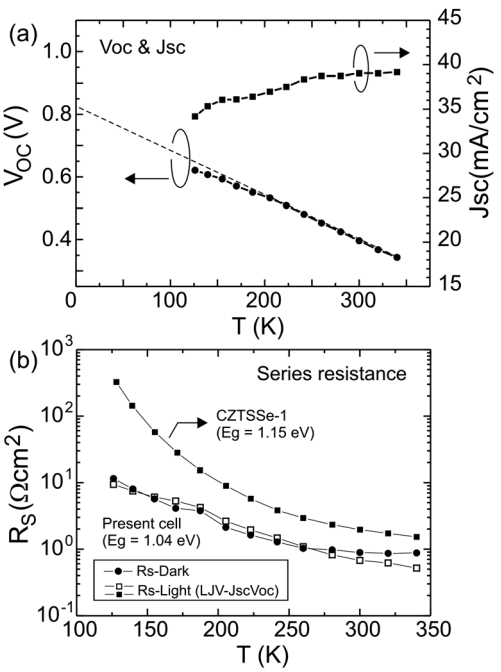

Fig. 3 (a) Voc and Jsc *vs.* temperature data under simulated 1 sun AM1.5G illumination (b) Temperature dependence data of the series resistance of the present cell and the previous champion cell CZTSSe-1.[10]

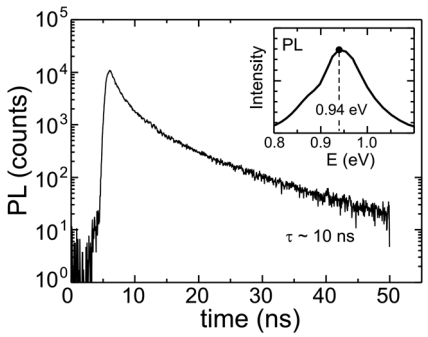

Fig. 4 Time-resolved photoluminescence data. Inset: PL spectrum showing a peak at λ = 0.94 eV where the TR-PL data is taken.

processed similarly to the record device (Fig. 5). At step 1, we have the initial completed CZTSe device with minority carrier lifetime in the range of 12 ns. In step 2, the completed CZTSe-B cell is placed in dilute hydrochloric acid for a minute to remove the top layers (*i.e.*, CdS, ZnO and ITO), thereby reverting the sample back to just the bare CZTSe absorber. Then we deposited CdS, ZnO and ITO layers again in steps 3–5, respectively. In contrast to ref. 26, we do not observe large variation in the minority carrier lifetime when a CZTSe film is coated with the additional CdS, ZnO and ITO layers. We therefore conclude that the lifetime measurements described above for the completed record device are reasonably representative of the bulk CZTSe film employed.

To study the series resistance characteristics of our cell we plot the temperature dependence data as shown in Fig. 3(b). Similar to our previous study,[10,20] we observe a significant increase in the series resistance at lower temperature. However this increase is notably less than the previous champion cell CZTSSe-1. Thus our present cell not only has smaller series resistance but also favorably weaker temperature dependence. Note that we measure the series resistance (R_S) both under dark and light conditions for comparison. The dark R_S is extracted using a method described in ref. 27 and the light R_S is extracted from the difference of the light J–V and the Jsc-Voc curves.[28] At high temperature (T > 260 K) the dark R_S is higher than the light R_S, as is usually observed concomitant with the cross-over behavior between dark and light J–V curves. This light-dependent R_S is often associated with electrical traps that get filled under illumination. However, at low temperature, both R_S values become large and similar in magnitude, suggesting that the root cause of the increase in series resistance is independent of light condition. The series resistance in CZTSSe, which is high and increasing at lower temperature, could be due to the presence of electrical barriers such as a non-ohmic back contact, buffer-absorber interface conduction band offset, carrier freeze-out effect or a combinations of the above. A more detailed understanding of this behavior is currently under investigation.

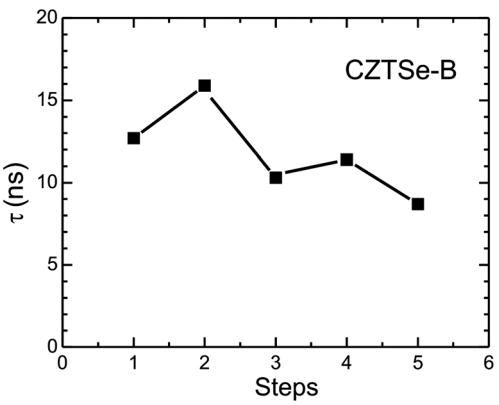

Fig. 5 Minority carrier lifetime after various processing steps for a CZTSe cell prepared similarly to the champion cell. Step 1 corresponds to a completed device. At step 2, the sample is placed in dilute hydrochloric acid for a minute to remove the top layers (*i.e.*, CdS, ZnO and ITO) and to revert the sample back to the bare CZTSe absorber. Then, CdS, ZnO and ITO are again successively deposited in steps 3–5.

Conclusion

In summary, we have synthesized a high performance low band gap CZTSe solar cell using solution-based processing. To date, the highest performing champion CZTSSe cells (independent of deposition approach) show efficiencies of 8.4% and 10.1% for a pure sulfur (CZTS)[29] and a mixed selenosulfur (CZTSSe) system,[10] respectively, with corresponding band gaps of 1.4 eV and 1.15 eV. Our current efficiency (10.1%) is the highest reported so far for low band gap CZTSe (Eg $\sim$ 1 eV). Compared to the previous higher band gap champion cell (also 10.1%, Eg = 1.15 eV), our current cell has lower Voc deficit with respect to the band gap, significantly longer minority carrier lifetime as measured by TRPL and lower series resistance. It is important to note that, in principle, the cell efficiency should increase with band gap until it reaches the theoretical optimum value of 1.45 eV for AM1.5G illumination. It is therefore interesting to note that, in the low band gap range of 1.0–1.2 eV, the current record efficiencies are identical. Despite this fact, it will be interesting to ascertain whether this similarity will be maintained as the efficiency records are pushed to higher values with increased device optimization.

Acknowledgements

This work was conducted as part of a joint development project between Tokyo Ohka Kogyo Co., Ltd., DelSolar Co., Ltd., Solar Frontier K. K. and IBM Corporation. The authors thank S. Jay Chey for deposition of ZnO and ITO and R. Ferlita for Ni/Al (and MgF_2) evaporation, Jemima Gonsalves for TEM sample preparation, and T. Goislard de Monsabert for assistance with high-accuracy PV device area measurement.

References

1 A. Shah, P. Torres, R. Tscharner, N. Wyrsch and H. Keppner, *Science*, 1999, **285**, 692.
2 P. Jackson, D. Hariskos, E. Lotter, S. Paetel, R. Wuerz, R. Menner, W. Wischmann and M. Powalla, *Progr. Photovolt.: Res. Appl.*, 2011, **19**, 894.
3 http://investor.firstsolar.com/releasedetail.cfm?ReleaseID=593994, accessed January 3, 2012.
4 http://www.miasole.com/sites/default/files/Cnet_Dec_02_2010.pdf, accessed January 3, 2012.
5 B. A. Andersson, *Progr. Photovolt.: Res. Appl.*, 2000, **8**, 61.
6 C. Wadia, A. P. Alivisatos and D. M. Kammen, *Environ. Sci. Technol.*, 2009, **43**, 2072.
7 H. Katagiri, *Tech. Dig. Photovoltaic Science and Engineering Conf.*, 1996, **9**, 745.
8 H. Katagiri, K. Jimbo, S. Yamada, T. Kamimura, W. S. Maw, T. Fukano, T. Ito and T. Motohiro, *Appl. Phys. Express*, 2008, **1**, 041201.
9 T. K. Todorov, K. B. Reuter and D. B. Mitzi, *Adv. Mater.*, 2010, **22**, E156.
10 D. A. R. Barkhouse, O. Gunawan, T. Gokmen, T. K. Todorov and D. B. Mitzi, *Progr. Photovolt.: Res. Appl.*, 2012, **20**, 6.
11 Q. Guo, G. M. Ford, W. C. Yang, B. C. Walker, E. A. Stach, H. W. Hillhouse and R. Agrawal, *J. Am. Chem. Soc.*, 2010, **132**, 17384.
12 W. Shockley and H. J. Queisser, *J. Appl. Phys.*, 1961, **32**, 510.
13 M. A. Contreras, K. Ramanathan, J. AbuShama, F. Hasoon, D. L. Young, B. Egaas and R. Noufi, *Progr. Photovolt.: Res. Appl.*, 2005, **13**, 209.
14 M. Contreras, J. Tuttle, D. Du, Y. Qi, A. Swartzlander, A. Tennant and R. Noufi, *Appl. Phys. Lett.*, 1993, **63**, 1824.

15 H. Wei, Z. Ye, M. Li, Y. Su, Z. Yang and Y. Zhang, *CrystEngComm*, 2011, **13**, 2222.
16 R. Haight, A. Barkhouse, O. Gunawan, B. Shin, M. Copel, M. Hopstaken and D. B. Mitzi, *Appl. Phys. Lett.*, 2011, **98**, 253502.
17 S. Chen, A. Walsh, J. H. Yang, X. G. Gong, L. Sun, P. X. Yang, J. H. Chu and S. H. Wei, *Phys. Rev. B: Condens. Matter Mater. Phys.*, 2011, **83**, 125201.
18 C. Persson and A. Zunger, *Appl. Phys. Lett.*, 2005, **87**, 211904.
19 M. J. Hetzer, Y. M. Strzhemechny, M. Gao, M. A. Contreras, A. Zunger and L. J. Brillson, *Appl. Phys. Lett.*, 2005, **86**, 162105.
20 O. Gunawan, T. K. Todorov and D. B. Mitzi, *Appl. Phys. Lett.*, 2010, **97**, 233506.
21 D. B. Mitzi, O. Gunawan, T. K. Todorov, K. Wang and S. Guha, *Sol. Energy Mater. Sol. Cells*, 2011, **95**, 1421.
22 K. Wang, O. Gunawan, T. Todorov, B. Shin, S. J. Chey, N. A. Bojarczuk, D. Mitzi and S. Guha, *Appl. Phys. Lett.*, 2010, **97**, 143508.
23 M. A. Green, *Sol. Cells*, 1982, **7**, 337.
24 V. Nadenau, U. Rau, A. Jasenek and H. W. Schock, *J. Appl. Phys.*, 2000, **87**, 584.
25 B. Ohnesorge, R. Weigand, G. Bacher, A. Forchel, W. Riedl and F. H. Karg, *Appl. Phys. Lett.*, 1998, **73**, 1224.
26 W. K. Metzger, I. L. Repins and M. A. Contreras, *Appl. Phys. Lett.*, 2008, **93**, 022110.
27 J. R. Sites and P. H. Mauk, *Sol. Cells*, 1989, **27**, 411.
28 D. Pysch, A. Mette and S. W. Glunz, *Sol. Energy Mater. Sol. Cells*, 2007, **91**, 1698.
29 B. Shin, O. Gunawan, N. Bojarczuk and S. Guha, *Progr. Photovolt.: Res. Appl.*, 2011, DOI: 10.1002/pip.1174.